

Isotope and temperature shifts of direct and indirect band gaps in diamond-type semiconductors

Stefan Zollner,* Manuel Cardona, and Sudha Gopalan

Max-Planck-Institut für Festkörperforschung, Heisenbergstrasse 1, D-7000 Stuttgart 80, Germany

(Received 17 June 1991)

We calculate the isotope and temperature shifts of the indirect and direct band gaps in natural silicon ($\bar{M}=28.09$ u), in natural diamond ^{12}C and its isotope ^{13}C , in natural germanium ($\bar{M}=72.59$ u), and the isotope ^{70}Ge , and in the isotope mixture $^{75,7}\text{Ge}$, due to the deformation-potential-type electron-phonon interaction (within the pseudopotential-bond-charge-model framework). We compare these results to existing experimental information and to data obtained by us with spectroscopic ellipsometry. We find that there are small, but noticeable shifts of the band gaps between different isotopes (about 13 meV for diamond, 1 meV for germanium). The isotopic influence on the broadenings of the E_1 transition in Ge is also reported.

I. INTRODUCTION

The conventional tetrahedral semiconductors Ge and Si can be grown as extremely good single crystals whose ultimate quality is determined by isotopic disorder due to the natural isotopic abundances (in natural germanium ^{70}Ge , 20.5%; ^{72}Ge , 27.4%; ^{73}Ge , 7.8%; ^{74}Ge , 36.5%; ^{76}Ge , 7.7%; in natural silicon ^{28}Si , 92%; ^{29}Si , 5%; ^{30}Si , 3%). The natural isotopic spread is less drastic, but still not negligible for diamond (^{12}C , 98.9%; ^{13}C , 1.1%). Small single crystals of isotopically enriched materials have been available for some time,¹⁻³ but are rather difficult to obtain. Recently, crystals of highly enriched ^{13}C diamonds, several mm in size, have been obtained and used in investigations of vibronic and electronic excitations.^{4,5} Also, isotopically enriched ^{12}C diamond has been shown to exhibit a remarkably high thermal diffusivity.⁶ Germanium is the tetrahedral material with the largest natural isotopic-mass spread and thus that in which effects of isotopic mass and isotopic disorder should be most easily observable. At the Kurchatov Institute in Moscow nearly isotopically pure (> 95%) germanium powders are being prepared in large amounts by standard isotope-separation techniques. From these materials germanium single crystals of high purity and perfection are being grown, in part because of their application as double- β -decay (^{76}Ge) and γ -ray detectors (^{70}Ge).⁷ These crystals, and that of ^{74}Ge which has been available for some time,² have been used to obtain interesting data on the dependence of the solid-state properties of germanium on isotopic mass and disorder. Among them we mention the decrease in thermal conductivity with increasing isotopic disorder,² the rather weak but non-negligible dependence of the lattice constant on isotopic mass,³ the dependence of phonon frequencies and linewidths on isotopic mass and disorder,^{8,9} and the dependence of electronic gaps on isotopic mass.^{10,11}

In this paper we present calculations of the dependence of several energy gaps and their Lorentzian widths

on isotopic mass for diamond, germanium, and silicon. We show that the effect is related to the dependence of the electron-phonon self-energy on isotopic mass and disappears at high temperatures as the average phonon amplitude becomes mass independent. As part of these calculations we also obtain the temperature dependence of the indirect and direct gaps of these materials. The theoretical results are compared with experimental data, in particular for the isotopic shifts of gaps recently obtained for germanium^{10,11} and diamond.⁵ Experimental data obtained ellipsometrically for the E_1 and $E_1 + \Delta_1$ transitions of natural Ge, ^{70}Ge , and ^{76}Ge are also presented. They contain information on the dependence of the gap frequency and Lorentzian widths on isotopic mass which compare favorably with the calculated results.

II. GENERAL THEORY OF TEMPERATURE SHIFTS

The deformation-potential electron-phonon interaction renormalizes the creation energies of electron-hole pairs (band gaps) thus causing shifts of the gaps with temperature. Small shifts are also introduced by the thermal expansion of the lattice. The theory for the temperature shifts in diamond-type semiconductors has been described in detail by Allen, Heine, Cardona, and Lautenschlager¹²⁻¹⁵ and reviewed by Cardona and Gopalan.¹⁶ For a review of earlier work, see Ref. 17. (The advantages and problems of the Allen-Heine or rigid-pseudoion method,¹² which we use here, have recently been discussed by Fischetti and Higman.¹⁸) This method describes the temperature shifts of the band gaps E_{CP} with three terms.

(i) By thermal expansion (TE) the lattice constant increases and thus the band gaps shrink, if they have a positive pressure coefficient $\partial E_{CP}/\partial p$. The shifts for the gaps are found to be¹⁷

$$\left(\frac{\partial E_{CP}}{\partial T}\right)_{\text{TE}} = -3\alpha(T)B \left(\frac{\partial E_{CP}}{\partial p}\right)_T, \quad (1)$$

where $\alpha(T)$ is the temperature-dependent thermal expansion coefficient and B the bulk modulus. In some cases (e.g., for the lowest indirect gap in Si), the pressure coefficient of the gap is negative and thus the TE contribution to the temperature shift is positive. This term can be evaluated very easily using the values listed in Table I and is small compared to those due to the electron-phonon interaction as described below.

(ii) The Debye-Waller term [see Fig. 1(a)] arises from the simultaneous interaction of an electron (with wave vector \mathbf{k} in band n) with two phonons of the same wave vector \mathbf{Q} and mode j (electron-two-phonon interaction). In the rigid-ion approximation we assume that the potential V_α of an atom of type α moves rigidly with the atom

$$(\Delta E_{n\mathbf{k}})_{\text{DW}} = \sum_{n',\mathbf{k}'} \sum_{\substack{\boldsymbol{\ell}\alpha \\ \boldsymbol{\ell}'\alpha'}} \frac{\mathbf{B}(n, \mathbf{k}, \boldsymbol{\ell}, \alpha, n', \mathbf{k}') \otimes \mathbf{B}(n', \mathbf{k}', \boldsymbol{\ell}', \alpha', n, \mathbf{k})}{-(E_{n\mathbf{k}} - E_{n',\mathbf{k}'})} : \langle \mathbf{u}_{\boldsymbol{\ell}\alpha} \otimes \mathbf{u}_{\boldsymbol{\ell}'\alpha'} \rangle^t, \quad (2)$$

where the sum runs over all intermediate electron states n', \mathbf{k}' , all lattice vectors $\boldsymbol{\ell}$, and the basis (α) of the lattice. The angular brackets with superscript t denote the thermal or temporal average. The energies necessary to distort the lattice (phonon energies) have been assumed to be much smaller than the usual electronic band gaps and thus are neglected in the denominator of Eq. (2). Thus

$$\mathbf{B}(n, \mathbf{k}, \boldsymbol{\ell}, \alpha, n', \mathbf{k}') = \langle n\mathbf{k} | \nabla V_\alpha(\mathbf{r} - \mathbf{R}_{\boldsymbol{\ell}\alpha}) | n'\mathbf{k}' \rangle \quad (3)$$

is the matrix element of the gradient of the potential V_α of one atom of type α located at the atomic site $\mathbf{R}_{\boldsymbol{\ell}\alpha}$. (The notation used here is somewhat symbolic, but very intuitive to emphasize the influence of the isotopic mass entering the phonon displacements $\mathbf{u}_{\boldsymbol{\ell}\alpha}$. For explicit expressions applicable for a lattice with a basis, see Ref. 15.) We use an empirical pseudopotential band structure and assume that the matrix element of the atomic potential with the true wave functions is the same as that

$$(\Delta E_{n\mathbf{k}})_{\text{SE}} = \sum_{n',\mathbf{k}'} \sum_{\substack{\boldsymbol{\ell}\alpha \\ \boldsymbol{\ell}'\alpha'}} \frac{\mathbf{B}(n, \mathbf{k}, \boldsymbol{\ell}, \alpha, n', \mathbf{k}') \otimes \mathbf{B}(n', \mathbf{k}', \boldsymbol{\ell}', \alpha', n, \mathbf{k})}{E_{n\mathbf{k}} - E_{n',\mathbf{k}'}} : \langle \mathbf{u}_{\boldsymbol{\ell}\alpha} \otimes \mathbf{u}_{\boldsymbol{\ell}'\alpha'} \rangle^t. \quad (4)$$

The imaginary part of this self-energy causes lifetime broadenings of critical points and is responsible for intervalley-scattering processes.²⁶

For numerical reasons, we Fourier-transform Eqs. (2) and (4) to the phonon representation (thus replacing the sum over lattice sites by an integration over all phonons in the first Brillouin zone) and label the contribution of a single phonon with wave vector \mathbf{Q} and branch j (with the occupation number $N_{\mathbf{Q}j}=1$) as $(\partial E_{n\mathbf{k}}/\partial N_{\mathbf{Q}j})_K$, where K stands for DW or SE. From these electron-phonon coupling coefficients we define the dimensionless electron-phonon spectral functions

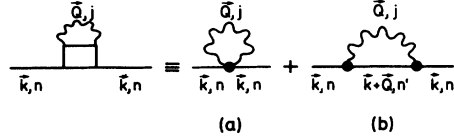


FIG. 1. Feynman diagrams for the renormalization of band gaps due to deformation potential-type electron-phonon interaction: (a) Debye-Waller term, (b) self-energy term.

in a phonon vibration. Then, the Debye-Waller (DW) contribution to the shifts of an electronic state $n\mathbf{k}$ for a frozen-in lattice displacement $\mathbf{u}_{\boldsymbol{\ell}\alpha}$ of one atom of type α located at the atomic site $\mathbf{R}_{\boldsymbol{\ell}\alpha}$ is given by^{17,15}

of the pseudopotential evaluated with the pseudo-wave-functions²⁴ (rigid pseudo-ion method). To second order in phonon displacement, Eq. (2) for the Debye-Waller term is equivalent to simply multiplying the structure factors $S(\mathbf{G})$ used in the band-structure calculations by Debye-Waller factors $\exp(-2W)$ with $W = \langle u^2 \rangle |\mathbf{G}|^2/12$. This term is the dominant contribution to the temperature shifts of band gaps. It has been evaluated for several materials in Ref. 25, but usually overestimates the shifts when considered without the other electron-phonon term discussed next.

(iii) The third contribution to the temperature shifts of electronic states is the real part of the self-energy (SE) term, which arises from the interaction of an electron with one phonon taken to second order in perturbation theory, see Fig. 1(b). This term is usually somewhat smaller than the Debye-Waller term, but opposite in sign. Therefore it should be taken into account in a realistic calculation of temperature shifts, although it requires a Brillouin-zone integration to be evaluated. It can be expressed as^{17,15}

TABLE I. Parameters needed for the evaluation of the thermal expansion contribution to the temperature shifts of band gaps (from Ref. 19, unless indicated by numbers in square brackets).

Material	Gap	$(\partial E/\partial p)_T$ (meV/GPa)	B (GPa)	α (300 K) (10^{-6} K^{-1})
Diamond	E'_0	7.0 [20]	442	1.0
	E_i	6.4 [21]		
	E_1	10		
Si	E_i	-14.1	98	2.56
	$\Gamma - L$	44 [22]		
Ge	$\Gamma - X$	-14 [23]	75	5.90

$$g^2 F_K(n, \mathbf{k}, \Omega) = \sum_{\mathbf{Q}_j} \left(\frac{\partial E_{n\mathbf{k}}}{\partial N_{\mathbf{Q}_j}} \right)_K \delta(\Omega - \Omega_{\mathbf{Q}_j}) \quad (5)$$

in such a way that the temperature shifts due to the DW or SE terms are given by

$$(\Delta E_{n\mathbf{k}})_K = \int_0^\infty d\Omega g^2 F_K(n, \mathbf{k}, \Omega) (N_\Omega + \frac{1}{2}). \quad (6)$$

For the integration over all phonon wave vectors \mathbf{Q} we use the tetrahedron method with 89 points in the irreducible wedge of the Brillouin zone.¹⁴

For the numerical evaluation of the terms in Eqs. (2) and (4) we assume that only the phonon amplitudes and not their energies depend on the temperature and isotope concentration. When calculating the energy denominators we neglect, for example, the small temperature dependence of the electron energies. (A self-consistent, iterative calculation is not necessary, since the shifts are much smaller than typical band gaps.) We use a constant imaginary self-energy of about 100 meV for the electrons to avoid numerical problems during the integration over all phonon wave vectors and to account for the finite lifetimes of the electronic states. We obtain the phonon energies and eigenvectors using Weber's bond-charge model.^{27,28} For the electronic structure and the evaluation of the matrix elements of Eq. (3) a local pseudopotential band structure with the form factors of Cohen and Bergstresser is used.²⁹ Similar form factors or lattice dynamical models yield analogous results. The accuracy of the method and the dependence of the matrix elements on different pseudopotential form factors have been discussed in detail in Refs. 18, 30, and 31.

An alternative formulation³² calculates the change in the phonon frequencies due to the interaction with electrons using a first-principle pseudopotential method.

III. TEMPERATURE SHIFTS

A. Diamond

Compared to other semiconductors, very little is known about the band structure of natural diamond ¹²C. Experimental investigations are made difficult by the large band gap (5.6 eV) calling for vacuum ultraviolet spectroscopies,³³⁻³⁶ whereas the lack of *p* electrons in the core and the tetrahedral distribution of the valence charge cause problems for pseudopotential band-structure calculations.³⁷⁻⁴⁰

In analogy to silicon, one should assume that the lowest conduction-band state at Γ is threefold degenerate and has Γ_{15} symmetry, in contrast to germanium (and most zinc-blende-type materials) which has a nondegenerate Γ_2' (*s**-like) conduction-band minimum. This is confirmed by photoemission measurements⁴¹ as well as quasiparticle energy calculations.^{42,43} Therefore, only the pseudopotential calculations of Refs. 39 and 37 seem to be realistic, although they result in dielectric functions which are in rather poor agreement with experiments.⁴⁰ Reflectivity measurements at 77 K and at room temperature suggest³⁶ that the direct gaps at Γ (E'_0) and along

Λ (E_1) are almost degenerate (just like in silicon), but this is still controversial⁴⁴ and has to be confirmed by further experiments or quasiparticle calculations. The lowest indirect gap occurs between the valence-band top at $\Gamma_{25'}$ and the conduction-band minimum along Δ near $(2\pi/a)(0.76, 0, 0)$ with an energy of about 5.6 eV, see Refs. 45 and 46.

In this investigation of the temperature shifts of critical points in diamond ¹²C, we have used the pseudopotential form factors of Ref. 39 which yield a band structure that is in reasonable overall agreement with experiments, when a plane-wave basis set with a cutoff of 17.4 Ry is taken for the calculation. The dimensionless electron-phonon spectral functions for the shifts of the E'_0 gap are shown in Fig. 2. The Debye-Waller term (dashed lines) is slightly larger for the valence band than for the conduction band, a fact which causes a decrease in the gap with increasing temperature. The self-energy term (solid lines) has a large negative optical-phonon peak for the conduction band and a positive peak for the valence band. It also causes a gap shrinkage, as shown in Fig. 3 (dashed-double-dotted line). The curves are qualitatively similar to those for silicon (see Figs. 4 and 5 in Ref. 14), but rather featureless in the acoustic-phonon energy range below 120 meV. This can be explained by differences in the one-phonon density of states of the two materials, see Fig. 8 of Ref. 27. The renormalization of the band gaps at 0 K, obtained by integrating Eq. (6) with N_Ω set to 0 for the different electronic states, is given in Table II. Since absolute shifts of states cannot be calculated with the empirical pseudopotential method, all shifts are measured with respect to the valence-band maximum at $\Gamma_{25'}$. These zero-point shifts will be dis-

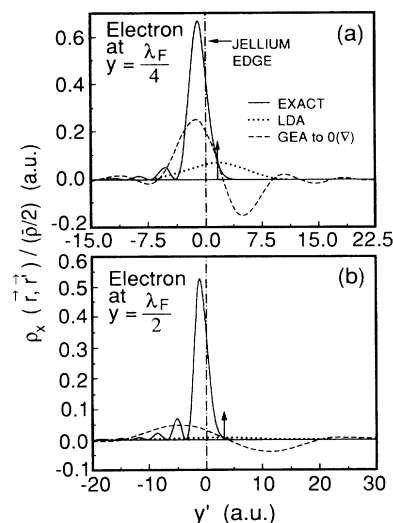


FIG. 2. Dimensionless electron-phonon spectral function $g^2 F$ for the shifts of the E'_0 gap in natural diamond ¹²C due to electron-phonon interaction as a function of phonon energy Ω . The Debye-Waller term (dashed line) is slightly larger for the valence band than for the conduction band. The optical phonon peak of the self-energy spectral function (solid line) is negative for the conduction band and positive for the valence band.

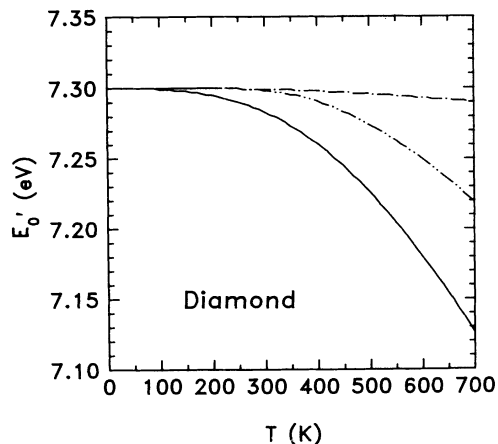


FIG. 3. Shifts of the E'_0 gap in natural diamond ^{12}C (solid line) including thermal expansion (dashed-dotted line), self-energy (dashed-double-dotted line), and Debye-Waller term (not shown separately). $E'_0(0\text{ K})=7.30$ eV has been assumed.

cussed in the isotope section of this paper.

The calculated energy of the E'_0 gap as a function of temperature (assuming $E'_0=7.3$ eV at 0 K), including all three contributions, is shown by the solid line in Fig. 3. The contributions of thermal expansion (dashed-dotted) and self-energy (dashed-double-dotted) are displayed separately. It can be seen that the shifts due to thermal expansion are small, especially because of the very small pressure dependence of the E'_0 gap commonly found in semiconductors.^{20,23,19} Furthermore, the TE contributions are rather small for all gaps in diamond

TABLE II. Renormalization of electronic states and band gaps due to the zero-point vibration of the phonons for two different isotopes of diamond (in meV, relative to the valence-band maximum).

State	Mass	SE	DW	Total
$\Gamma_{25'}(v)$	12.00	0.0	0.0	0.0
$\Gamma_{15}(c)$	12.00	-547.8	-130.1	-677.9
$\Delta_5(v)$	12.00	-401.2	-46.9	-448.1
$\Delta_1(c)$	12.00	-441.5	-177.4	-619.0
$L_{3'}(v)$	12.00	-43.1	-11.6	-54.7
$L_1(c)$	12.00	-409.5	-253.6	-663.1
E'_0	12.00	-547.8	-130.1	-677.9
E_{ind}	12.00	-441.5	-177.4	-619.0
$E_2(\Delta)$	12.00	-40.3	-130.5	-170.9
$E_1(L)$	12.00	-366.4	-242.0	-608.4
$\Gamma_{25'}(v)$	13.00	0.0	0.0	0.0
$\Gamma_{15}(c)$	13.00	-531.3	-125.2	-656.3
$\Delta_5(v)$	13.00	-391.0	-45.2	-436.1
$\Delta_1(c)$	13.00	-431.1	-170.8	-601.9
$L_{3'}(v)$	13.00	-44.9	-11.2	-56.0
$L_1(c)$	13.00	-399.9	-244.1	-644.0
E'_0	13.00	-531.3	-125.2	-656.3
E_{ind}	13.00	-431.1	-170.8	-601.9
$E_2(\Delta)$	13.00	-40.1	-125.6	-165.8
$E_1(L)$	13.00	-355.1	-232.9	-588.0

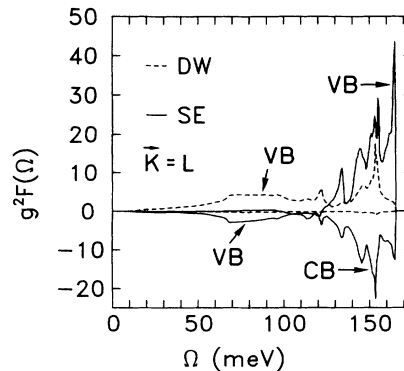


FIG. 4. As Fig. 2, but for the gap at L in diamond ^{12}C . The magnitude of the DW and SE terms is larger for the valence bands than for the conduction bands.

because of the large bulk modulus (442 GPa, see Ref. 21). The Debye-Waller contribution is dominant up to about 400 K, but at 700 K the self-energy accounts for 40% of the shifts. The only experimental data for the shifts of the E'_0 gap in diamond known to us are the reflection measurements of Clark, Dean, and Harris⁴⁵ reporting a shift of the direct gap of 100 meV between 133 and 295 K. This result is much larger than our calculated shifts (only 15 meV), but it is not clear whether the assignment of the experimental peak to E'_0 transitions is correct. In silicon, the E'_0 and E_1 critical points are almost degenerate.⁴⁷ Since the shifts become sizable at elevated temperatures, reflectivity measurements should be performed up to 700 K.

In order to be able to distinguish between the E'_0 and E_1 critical points, we have also calculated the shifts at L and three points along Λ between Γ and L . The electron-phonon spectral function for $\mathbf{k} = L$ in diamond is shown in Fig. 4. The various peaks in the self-energy term for the optical phonons correspond to $\text{LO}(X)$ (132 meV), $\text{TO}(X)$ (147 meV), $\text{LTO}(L)$ (150 meV), and $\text{LTO}(\Gamma)$ (165 meV). An increase of the mesh used in the integration over all phonon wave vectors from 89 points to

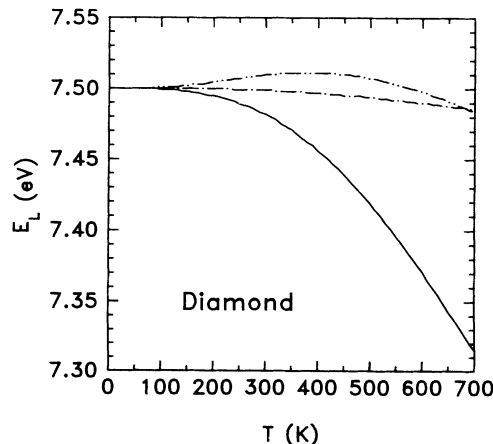


FIG. 5. As Fig. 3, but for the gap at L in diamond ^{12}C . $E_L(0\text{ K})=7.50$ eV has been assumed.

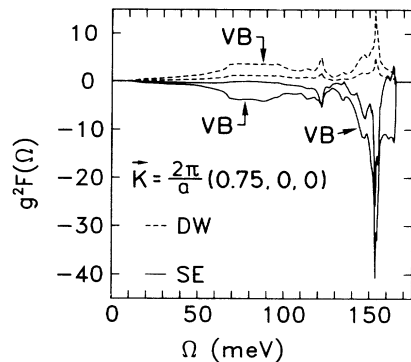


FIG. 6. As Fig. 2, but for the point $\mathbf{k} = (0.75, 0, 0) (2\pi/a)$ in diamond ^{12}C . The magnitude of DW and SE terms is larger for the valence band than for the conduction band.

505 points in the irreducible wedge of the Brillouin zone does not change the spectral function significantly. The electron-phonon contributions to the shifts of the direct gaps are almost equal at Γ and L , but slightly smaller (by about 15%) along Λ . For the calculation of the thermal expansion term we need the pressure coefficient of the gap at L , but no such calculation exists to our knowledge. Setting $a(E_1) = -4.4$ eV seems to be a good guess,²² implying $\partial E_1/\partial p = 10$ meV/GPa. We thus show the temperature dependence of the gap at L in Fig. 5, assuming it to be 7.5 eV at 0 K. For this gap, the contribution of the DW term is dominant, similar to the case of GaSb (see Fig. 10 of Ref. 48).

The spectral functions for the $\Gamma_{25'}$ valence band (Fig. 2) and for the conduction band at the point $\mathbf{k} = (0.75, 0, 0) \times (2\pi/a)$ (see Fig. 6) were used to calculate the temperature dependence of the indirect gap E_i of diamond (see Fig. 7). $E_i(0 \text{ K}) = 5.41$ eV has been assumed. As in the previous figures, the solid line shows the total calculated shifts including thermal expansion (dashed-dotted line), self-energy (dashed-double-dotted line), and Debye-Waller term (not given explicitly). It can be seen that the Debye-Waller term dominates the

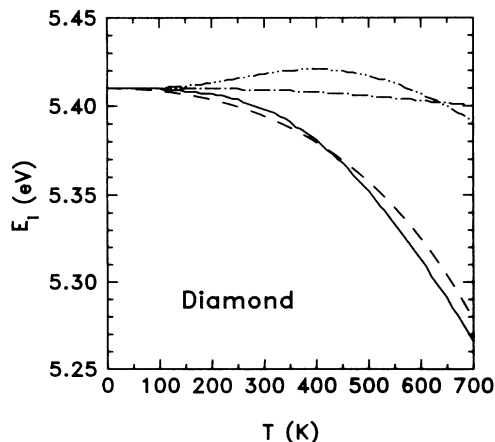


FIG. 7. As Fig. 3, but for the lowest indirect gap in diamond ^{12}C . $E_i(0 \text{ K}) = 5.41$ eV has been assumed. The dashed line shows the experimental data of Ref. 45.

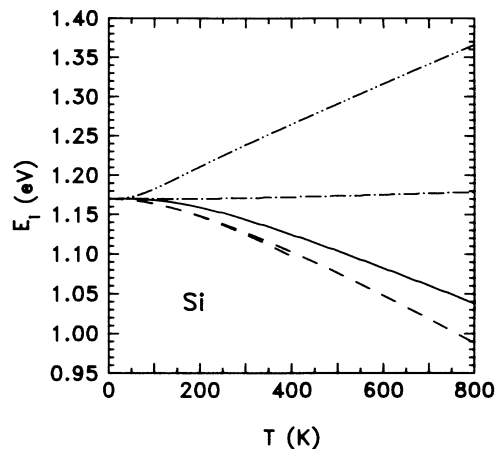


FIG. 8. As Fig. 3, but for the lowest indirect gap in silicon. $E_i(0 \text{ K}) = 1.17$ eV has been assumed. The dashed lines show the experimental data of Ref. 50 (up to 400 K) and of Ref. 49 (up to 800 K).

shifts, in contrast to the results for the E'_0 critical point (see Fig. 3). We also show the experimental data of Clark, Dean, and Harris⁴⁵ (dashed line), which are in good agreement with our calculated results.

B. Silicon

A comparison of the experimental and theoretical data for the temperature dependence of the band gaps of silicon has been performed by Lautenschlager and co-workers.^{15,47} Further experimental data, however, have become available for the lowest indirect gap.⁴⁹ We therefore show a comparison of these data and those of Thurmond⁵⁰ with our calculated results in Fig. 8. We should point out that calculations also have been carried out by King-Smith *et al.*³²

We have also calculated the temperature dependence of the second lowest indirect gap $\Gamma_{25'} \rightarrow L_1$, see Fig. 9. Although silicon is the best studied semiconductor, the exact energy of this transition is not well known. Forman, Thurber, and Aspnes⁵¹ report $E(\Gamma_{25'} \rightarrow L_1) = 1.65$

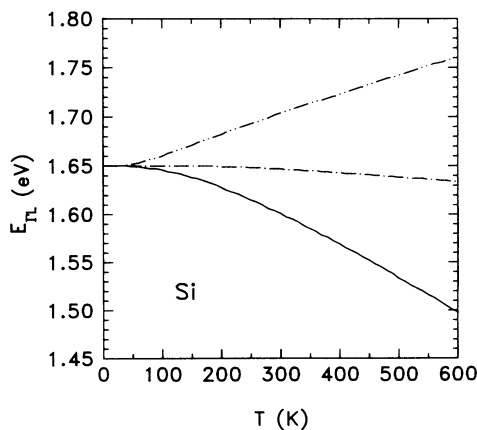


FIG. 9. As Fig. 3, but for the second indirect gap $\Gamma_{25'}(v) \rightarrow L_1(c)$ in silicon.

eV (which is consistent with linear-muffin-tin-orbital calculations²² of the position of the valence band at L and the value of the E_1 gap in silicon⁴⁷), but other groups have not been able to reproduce these measurements.⁵² Recent angle-resolved-photoemission measurements,^{53,54} another optical experiment,⁵⁵ most *ab initio* pseudopotential band-structure calculations⁵⁶ (in conjunction with the ellipsometric result for E_1), as well as quasiparticle energy calculations^{57,43} place this transition about 0.5–0.7 eV higher in energy.

C. Germanium

The temperature dependence of the lowest indirect [$\Gamma_{25'}(v) \rightarrow L_1(c)$] and various direct gaps has been calculated in Refs. 14 and 15. For completeness, we give in Fig. 10 the temperature dependence of the indirect gap between $\Gamma_{25'}(v)$ and $X_1(c)$ which is important for the transport properties of germanium. Based on photoemission data⁴⁴ we take this transition to have an energy of 1.30 eV at 0 K, a value somewhat higher than that from the quasiparticle band-structure calculations,^{42,58} but in excellent agreement with the more recent results of Hott.⁴³ The photoluminescence measurements of silicon-germanium alloys (extrapolated to pure germanium) by Weber and Alonso⁴⁹ suggest $X_1^c=0.93$ eV.

IV. ISOTOPE SHIFTS

It can be seen that at a given temperature T isotope effects enter in Eqs. (2) and (4) through the mean-squared phonon amplitude

$$\langle \mathbf{u}_{\mathbf{Q}j}^2 \rangle^t = \frac{\hbar^2}{2M_\alpha N \Omega_{\mathbf{Q}j}} [1 + 2N_{\mathbf{Q}j}(T)], \quad (7)$$

where M_α is the mass of one atom of type α and $N_{\mathbf{Q}j}(T)$ the occupation number of the phonon with wave vector \mathbf{Q} , branch j , and energy $\Omega_{\mathbf{Q}j}$. We neglect the small isotope dependence of the matrix elements of Eq. (3). Therefore, Debye-Waller and self-energy terms not only

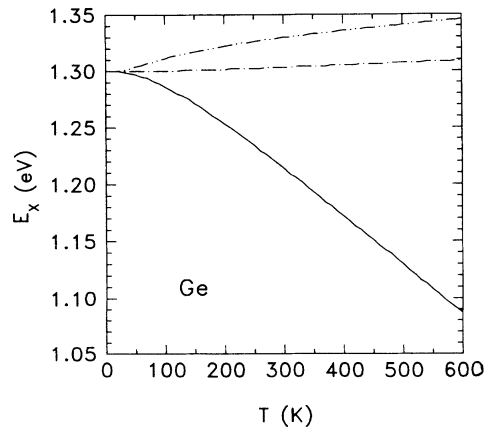


FIG. 10. As Fig. 3, but for the second indirect gap $\Gamma_{25'}(v) \rightarrow X_1(c)$ in germanium.

cause temperature shifts, but also an isotope-dependent renormalization of the electron energies at zero temperature. At 0 K (when $N=0$), we have

$$\langle \mathbf{u}_{\mathbf{Q}j}^2 \rangle^t \propto M_\alpha^{-1/2}, \quad (8)$$

since the phonon frequencies are proportional to $M_\alpha^{-1/2}$.

We mention briefly that (in analogy to the thermal expansion contribution to the temperature shifts) there is a third term in the isotope shifts not due to electron-phonon interaction.^{3,5,10} If the atoms in a crystal are replaced by heavier isotopes, the anharmonic contribution to the vibrational energy decreases. In order to compensate this decrease, the crystal contracts thus minimizing the total free energy. Typical volume changes are about 10^{-3} for carbon (between ^{12}C and ^{13}C) and 10^{-5} for germanium (between ^{70}Ge and ^{76}Ge).³ We will not discuss these shifts here, as they are usually at least an order of magnitude smaller than the isotopic shifts due to electron-phonon interaction.^{5,10}

A. Diamond

Natural diamond has an atomic weight of 12.01 and consists of the isotope ^{12}C with traces of ^{13}C . Nevertheless, synthetic growth of crystals of ^{13}C , up to 3 mm in diameter, has been reported in the literature.^{4,5} From Table II it can be seen that the renormalization of the gaps due to electron-phonon interaction is rather large [near 600 meV, except for $E_2(\Delta)$]. The magnitudes of these corrections to the gaps are larger for the lighter isotope ^{12}C , scaling approximately as $M_\alpha^{-1/2}$, as predicted by Eq. (8). Therefore, the measured gaps are larger for ^{13}C than for ^{12}C . We predict energy differences of 21.6, 5.1, and 20.4 meV for the direct gaps E'_0 , $E_2(\Delta)$, and $E_1(L)$, respectively. For the lowest indirect gap an isotope shift of 14 ± 0.7 meV was found by Collins *et al.*,⁵ in rather good agreement with our calculated result (17.1 meV). We stress that our formalism contains no free parameters for the electron-phonon coupling. (The size of the plane-wave basis set in principle is a free parameter, but its influence on the band structure as well as the temperature or isotope shifts in most cases is smaller than 10% and therefore negligible.) The parameters for the electronic band structure and the phonon frequencies and eigenvectors were taken from the literature without adjustment.^{39,27}

The Debye-Waller term gives the main contribution to the zero-point renormalizations, whereas the self-energy accounts only for about 20–40%, except for the $E_2(\Delta)$ gap where it gives the dominant contribution. The same statement holds, of course, for the contributions to the isotopic differences.

It is also of interest to study the influence of the atomic mass on the temperature shifts discussed earlier. If $k_B T$ is much larger than the phonon energies of a material, N becomes independent of M and the shifts should not depend on the isotope. This approximation will certainly not hold at moderate temperatures for diamond with its large phonon energies of up to 165 meV. Therefore, a small isotope dependence of the temperature shifts is ex-

pected. We calculate indeed that the indirect gap in natural diamond ^{12}C shifts down by 11.0 meV from 0 to 300 K and by 12.0 meV in ^{13}C . Therefore, the isotopic effect on the indirect gap should be smaller by 1 meV at room temperature than at 0 K. Similar results were obtained for the direct gaps E'_0 and $E_1(L)$.

B. Germanium

Natural germanium contains five different isotopes ($M = 70, 72, 73, 74,$ and 76) with an average atomic mass of $M=72.59$. Nearly isotopically pure ^{70}Ge and ^{74}Ge , as well as crystals containing two isotopes with an average mass of $M=75.69$, have been grown by different groups.^{2,8,10}

The zero-point renormalization energies for three crystals with $M=70.00, 72.59,$ and 75.69 are given in Table III. We conclude that the indirect gap in natural germanium should have an energy that is 1.3 meV lower than in a germanium crystal with $M=75.69$. In a recent experiment,¹⁰ this isotope shift has been measured to be 0.9 ± 0.1 meV, in reasonable agreement with our calculations. By the same token, we calculate an isotope shift of 1.4 meV for the direct gap, whereas 1.25 ± 0.05 meV

TABLE III. As Table II, but for three germanium crystals with different atomic masses.

State	Mass	SE	DW	Total
$\Gamma_{25'}(v)$	70.00	0.0	0.0	0.0
$\Gamma_2(c)$	70.00	-27.50	-34.92	-62.42
$L_{3'}(v)$	70.00	-4.08	-4.91	-8.99
$L_1(c)$	70.00	-22.80	-34.66	-57.46
$X_4(v)$	70.00	-22.74	-11.38	-34.12
$X_1(c)$	70.00	-23.35	-37.30	-60.65
E_0	70.00	-27.50	-34.92	-62.42
$E_{\Gamma L}$	70.00	-22.80	-34.66	-57.46
$E_1(L)$	70.00	-18.72	-29.75	-48.47
$E_2(X)$	70.00	-0.61	-25.92	-26.53
$\Gamma_{25'}(v)$	72.59	0.0	0.0	0.0
$\Gamma_2(c)$	72.59	-27.18	-34.33	-61.51
$L_{3'}(v)$	72.59	-4.02	-4.82	-8.84
$L_1(c)$	72.59	-22.55	-34.07	-56.62
$X_4(v)$	72.59	-22.48	-11.19	-33.67
$X_1(c)$	72.59	-23.10	-36.67	-59.77
E_0	72.59	-27.18	-34.33	-61.51
$E_{\Gamma L}$	72.59	-22.55	-34.07	-56.62
$E_1(L)$	72.59	-18.53	-29.25	-47.78
$E_2(X)$	72.59	-0.62	-25.48	-26.10
$\Gamma_{25'}(v)$	75.69	0.0	0.0	0.0
$\Gamma_2(c)$	75.69	-26.54	-33.54	-60.08
$L_{3'}(v)$	75.69	-4.00	-4.72	-8.72
$L_1(c)$	75.69	-22.05	-33.29	-55.34
$X_4(v)$	75.69	-21.93	-10.94	-32.87
$X_1(c)$	75.69	-22.56	-35.83	-58.39
E_0	75.69	-26.54	-33.54	-60.08
$E_{\Gamma L}$	75.69	-22.05	-33.29	-55.34
$E_1(L)$	75.69	-18.05	-28.57	-46.62
$E_2(X)$	75.69	-0.63	-24.89	-25.52

was found experimentally.¹⁰

In contrast to diamond, self-energy and Debye-Waller terms contribute almost equally to the zero-point renormalization and isotope shifts. Therefore, the self-energy terms have to be included for a reasonable theoretical estimate of the changes in electronic energies due to electron-phonon interactions. Just as for diamond, the isotopic shifts decrease with increasing temperature.

V. EXPERIMENTS

In this section we discuss ellipsometric measurements of the E_1 and $E_1 + \Delta_1$ gaps of various isotopes of germanium. The data were obtained for three n -type crystals with isotopic composition given in Table IV. Two of them (natural Ge and enriched ^{76}Ge) were intrinsic at room temperature ($N_d - N_a \sim 10^{14} \text{ cm}^{-3}$, obtained from Hall measurements) and had gone through a stringent purification procedure during growth. The third sample (^{70}Ge) contained a larger concentration of donors and acceptors, with $N_d - N_a \sim 7 \times 10^{16} \text{ cm}^{-3}$. The electrical measurements were confirmed by far-infrared transmission. As shown by Viña and Cardona,⁵⁹ the free-carrier concentration caused by the doping in these samples is too small to have any measurable effect on the ellipsometric spectra.

A. Results

The spectroscopic ellipsometry measurements of the three Ge samples in Table IV were performed at 10 K and at room temperature inside a cryostat with quartz windows nearly free of birefringence. The reflecting surfaces were (111)-oriented and polished and etched using the procedure described in Refs. 60 and 61 immediately before mounting them in the cryostat. The data obtained were similar to those of Refs. 60 and 61 and are shown in Fig. 11.

By comparing our spectrum at 300 K (not shown in Fig. 11) with the data of Aspnes and Studna⁶⁰ at the peak of ϵ_2 at 4.35 eV, we find that our samples are covered with a thin oxide layer of 0.9 nm thickness. After correcting our spectrum for such an overlayer (dashed line) we obtain good agreement with the data of Ref. 60. The dotted line shows a spectrum taken at 10 K (uncorrected), the solid line the same spectrum after correction for 0.9 nm of GeO_2 oxide. On this scale, no differences can be found between the different isotopes.

TABLE IV. Isotopic composition of enriched ^{70}Ge , ^{76}Ge , and natural Ge used in the ellipsometric experiments. g represents the mean square mass fluctuation defined in Ref. 11.

M	Atomic percent of the various isotopes					g (10^{-5})
	70	72	73	74	76	
^{70}Ge	95.9	3.8				2.976
$^{72.6}\text{Ge}$	20.5	27.4	7.8	36.5	7.1	58.745
$^{75.6}\text{Ge}$		0.1	0.23	13.7	86.0	8.797

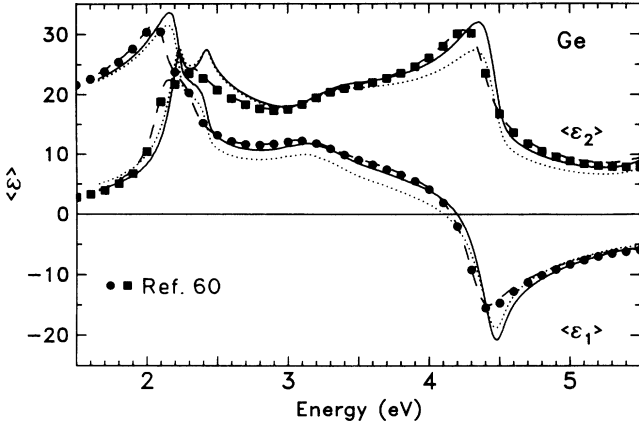


FIG. 11. Dielectric function of natural Ge at 300 K as obtained by Aspnes and Studna (Ref. 60) (symbols) and in this work after a correction for an oxide layer of 0.9 nm thickness (dashed line). The dotted line shows an uncorrected spectrum at 10 K, the solid line the same spectrum after a correction for 0.9-nm oxide. Isotopic differences between the three samples (see Table IV) are not visible on this scale.

In order to precisely determine the energies of the E_1 and $E_1 + \Delta_1$ critical points, we calculated numerically the third derivative of our spectra and performed a line-shape analysis as described in detail in Ref. 48. Two-dimensional critical points were used to describe the observed line shape. The best fits to the spectra taken for the three samples are shown in Fig. 12. It can be seen that there is indeed a small shift (of the same order as our error bars obtained from measuring the same sample several times), with the heaviest isotope having the highest energy.

B. Discussion

The energies of the critical points E_1 and $E_1 + \Delta_1$ and their Lorentzian widths were obtained from the fits to the derivative spectra shown in Fig. 12. They are listed in Table V. The mass dependence of the Γ 's can easily be estimated from the measured temperature dependence of Γ . Such an estimate is more difficult for the isotopic shift of E_1 and $E_1 + \Delta_1$. The reason is that the observed widths Γ are actually due fully to electron-phonon interaction while the contribution of this interaction to E_1 and

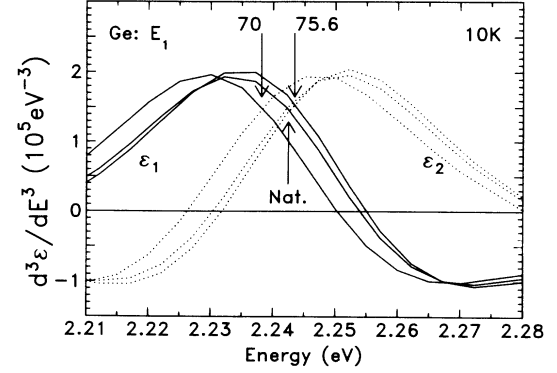


FIG. 12. Fits to the third derivative spectra of the real (ϵ_1 , solid line) and imaginary (ϵ_2 , dotted line) parts of the dielectric function of three germanium samples with different isotopic compositions (indicated by the arrows) around the E_1 critical point taken at 10 K. The vertical arrows show the positions of the critical-point energies as determined from a line shape analysis. The spectra have been multiplied with factors close to unity (0.8, . . . , 1.2) so as to exhibit the same amplitude.

$E_1 + \Delta_1$ cannot be *directly* inferred from experiment. It must be estimated through a fit of the measured temperature dependence of E_1 and $E_1 + \Delta_1$ and is thus strongly affected by the functions taken for the fit.⁴⁷ From (7) and the widths of Table V we obtain directly the isotopic shifts in Γ with respect to those of the natural material given in Table V. We recall that the measured values of Γ agree reasonably well with those calculated using a realistic pseudopotential band structure and a lattice dynamics based on the bond charge model.¹⁵

The interpretation of the measured δE_1 and $\delta(E_1 + \Delta_1)$ must be made by comparison with the calculated values at $T = 0$ due to the zero-point vibrational amplitudes.¹⁵ We find $\delta E_1 \approx \delta(E_1 + \Delta_1) = 58$ meV averaged over the $\langle 111 \rangle$ points at which the E_1 and $E_1 + \Delta_1$ transitions occur [no spin-orbit splitting was included in these calculations, a fact which we now know does not significantly alter the values of δE (Ref. 15)]. From this value of the zero-point vibrational effect on the gap energy and Eq. (8) we find those of $\delta E_1 \approx \delta(E_1 + \Delta_1)$ listed in Table V.

It is strikingly apparent in Table V that while the measured values of δE_1 and $\delta(E_1 + \Delta_1)$ for ^{76}Ge agree,

TABLE V. Energies and Lorentzian widths (half-width at half maximum) of the E_1 and $E_1 + \Delta_1$ critical points of two isotopically enriched Ge samples (see Table IV) and a natural one. The corresponding changes in self-energy δE , $\delta \Gamma$ are referred to the natural sample.

\bar{M}	E_1 (meV)	$E_1 + \Delta_1$ (meV)	Γ_{E_1} (meV)	$\Gamma_{E_1 + \Delta_1}$ (meV)	δE_1 (meV)	$\delta \Gamma_i(E_1)$ (meV)	$\delta(E_1 + \Delta_1)$ (meV)	$\delta \Gamma_i(E_1 + \Delta_1)$ (meV)				
70	2237.8(6)	2435.4(4)	35.1(3)	38.0(3)	-4.4(18) ^a	-1 ^b	2.1(4) ^a	0.5 ^b	-4.9(12) ^a	-1 ^b	1.9(8) ^a	0.6 ^b
72.6	2242.2(17)	2440.3(12)	33.0(3)	36.1(7)	0	0	0	0	0	0	0	0
75.6	2243.3(5)	2441.3(4)	32.6(2)	35.5(5)	1.1(18) ^a	1.35 ^b	-0.4(4) ^a	-0.8 ^b	1.0(12) ^a	1.35 ^b	-0.6(9) ^a	-0.8 ^b

^aExperimental.

^bCalculated.

within the admittedly large error bars, with the calculated ones, those for ^{70}Ge are considerably larger (approximately a factor of 4) although they have the correct sign predicted by the isotopic-shift theory. Since this sign is that which corresponds to increasing thermal agitation, i.e., disorder (the ^{70}Ge atoms vibrate with larger amplitude than the natural material $^{72.6}\text{Ge}$) we conjecture that our ^{70}Ge material contains a larger concentration of impurities than the other two samples known to have $N_D \simeq 10^{14} \text{ cm}^{-3}$. The ^{70}Ge had not gone through the stringent purification process to which the other two samples had been subjected. We actually know that for our ^{70}Ge , $N_D - N_A \simeq 7 \times 10^{16} \text{ cm}^{-3}$. In the absence of compensation (i.e., $N_A \ll N_D$) the corresponding donor concentration would have an unobservable effect on the E_1 and $E_1 + \Delta_1$ energies ($\lesssim 0.5 \text{ meV}$) and the corresponding broadenings $\Gamma = -\Sigma_i (i \lesssim 0.5 \text{ meV})$.⁵⁹ We conclude that this sample must be strongly compensated (a conclusion supported by ir-transmission data), with $N_D \simeq N_A = 5 \times 10^{17} \text{ cm}^{-3}$.⁵⁹ We note the possibility of using disorder-induced critical point shifts for an estimate of the degree of compensation in samples for which N_D and N_A are not separately known.

VI. CONCLUSIONS

We have calculated the temperature dependence of the energy and Lorentzian widths of electronic states at several high-symmetry points of the Brillouin zone for diamond, silicon, and germanium. We have shown that

the effects of the zero-point vibrations ($T = 0$) are by no means negligible and result in the dependence of the gaps on isotopic mass at low temperature. This effect should be important when comparing gaps theoretically calculated for a static lattice with the measured ones, in view of the increasing reliability and accuracy of such calculations.^{43,42} The calculated temperature shifts of several gaps have been found to account well for the experimental results. Also, recently measured effects of the isotopic mass on several gaps of diamond and germanium have been shown to agree with our theoretical predictions.

ACKNOWLEDGMENTS

The original versions of the computer code used in this study were written by P. B. Allen, P. Lautenschlager, and L. Viña. The Hall measurements to determine the carrier concentrations of the germanium samples were kindly performed by P. O. Hansson. We are thankful to V. Ozogin for supplying the raw ^{70}Ge powder and to E. E. Haller, W. L. Hansen, and K. Itoh for growing the ^{70}Ge single crystal. Thanks are also due to S. T. Belyaev, H. V. Klapdor-Kleingrothaus, and U. Schmidt-Rohr, of the Heidelberg-Moscow solar neutrino project, for the loan of the ^{76}Ge crystal. Expert technical help by M. Siemers, P. Wurster, H. Hirt, G. Schneider, and W. Stiepany is also gratefully acknowledged. The authors are thankful for partial support from the "Fonds der Chemischen Industrie, Frankfurt."

*Present address: International Business Machines Corporation, Thomas J. Watson Research Center, P. O. Box 218, Yorktown Heights, NY 10598. Electronic mail: STZO@VAXFF1.MPI-STUTTGAERT.MPG.DE.

¹G. Feher, J. P. Gordon, E. A. Gere, and C. D. Thurmond, *Phys. Rev.* **108**, 221 (1958).

²T. H. Geballe and G. H. Hull, *Phys. Rev.* **110**, 773 (1958).

³R. C. Buschert, A. E. Merlino, S. Pace, S. Rodriguez, and M. H. Grimsditch, *Phys. Rev. B* **38**, 5219 (1988).

⁴A. T. Collins, G. Davies, H. Kanda, and G. S. Woods, *J. Phys. C* **21**, 1363 (1988).

⁵A. T. Collins, S. C. Lawson, G. Davies, and H. Kanda, *Phys. Rev. Lett.* **65**, 891 (1990).

⁶T. R. Anthony, W. F. Bauholzer, J. F. Fleischer, L. Wei, P. K. Kuo, R. L. Tomas, and R. W. Pryor, *Phys. Rev. B* **42**, 1104 (1990).

⁷K. Grotz and H. V. Klapdor-Kleingrothaus, *The Weak Interaction in Nuclear Particle and Astrophysics* (Hilger, Bristol, 1990); N. Gehrels, *Nucl. Instrum. Methods A* **292**, 505 (1990).

⁸H. D. Fuchs, C. H. Grein, C. Thomsen, M. Cardona, W. L. Hansen, and E. E. Haller, *Phys. Rev. B* **43**, 4835 (1991).

⁹H. D. Fuchs, C. H. Grein, R. I. Devlen, J. Kuhl, and M. Cardona, *Phys. Rev. B* **44**, 8633 (1991).

¹⁰V. F. Agekyan, V. M. Asnin, A. M. Kryukov, I. I. Markov, N. A. Rud', V. I. Stepanov, and A. B. Curilov, *Fiz. Tverd. Tela (Leningrad)* **31**, 101 (1989). [*Sov. Phys. Solid State* **31**, 2082 (1989)].

¹¹M. Cardona, C. H. Grein, H. D. Fuchs, and S. Zollner, *J.*

Non-Cryst. Solids (to be published).

¹²P. B. Allen and V. Heine, *J. Phys. C* **9**, 2305 (1976).

¹³P. B. Allen and M. Cardona, *Phys. Rev. B* **23**, 1495 (1981); **24**, 7479 (1981).

¹⁴P. B. Allen and M. Cardona, *Phys. Rev. B* **27**, 4760 (1983).

¹⁵P. Lautenschlager, P. B. Allen, and M. Cardona, *Phys. Rev. B* **31**, 2163 (1985); S. Gopalan, P. Lautenschlager, and M. Cardona, *ibid.* **35**, 5577 (1987).

¹⁶M. Cardona and S. Gopalan, in *Progress on Electron Properties of Solids*, edited by R. Girlanda (Kluwer, Dordrecht, The Netherlands, 1989), p. 51.

¹⁷M. L. Cohen and D. J. Chadi, in *Handbook of Semiconductors*, edited by M. Balkanski (North-Holland, Amsterdam, 1980), Vol. 2, p. 155.

¹⁸M. V. Fischetti and J. M. Higman, in *Monte Carlo Device Simulation: Full Band and Beyond*, edited by K. Hess (Kluwer, Norwell, MA, 1991), p. 123.

¹⁹O. Madelung, in *Numerical Data and Functional Relationships in Science and Technology*, edited by O. Madelung (Springer, Berlin, 1987), Vols. 17a and 22a.

²⁰M. Cardona and N. E. Christensen, *Solid State Commun.* **58**, 421 (1986).

²¹P. E. Van Camp, V. E. Van Doren, and J. T. Devreese, *Phys. Rev. B* **34**, 1314 (1986).

²²U. Schmid, N. E. Christensen, and M. Cardona, *Solid State Commun.* **75**, 39 (1990).

²³K. J. Chang, S. Froyen, and M. L. Cohen, *Solid State Commun.* **50**, 105 (1984).

²⁴L. J. Sham, *Proc. Phys. Soc. London* **78**, 895 (1961).

- ²⁵J. Camassel and D. Auvergne, *Phys. Rev. B* **12**, 3258 (1975).
- ²⁶S. Zollner, S. Gopalan, M. Garriga, J. Humlíček, L. Viña, and M. Cardona, *Appl. Phys. Lett.* **57**, 2838 (1990).
- ²⁷W. Weber, *Phys. Rev. B* **15**, 4789 (1977); O. H. Nielsen and W. Weber, *Comput. Phys. Commun.* **18**, 101 (1979).
- ²⁸D. Strauch, A. P. Mayer, and B. Dorner, *Z. Phys. B* **78**, 405 (1990).
- ²⁹M. L. Cohen and T. K. Bergstresser, *Phys. Rev.* **141**, 789 (1966).
- ³⁰S. Zollner, Sudha Gopalan, and M. Cardona, *J. Appl. Phys.* **68**, 1682 (1990).
- ³¹Stefan Zollner, Ph.D. thesis, Max-Planck-Institut für Festkörperforschung, Stuttgart, Germany, 1991.
- ³²R. D. King-Smith, R. J. Needs, V. Heine, and M. J. Hodgson, *Europhysics Lett.* **10**, 569 (1989); R. D. King-Smith and R. J. Needs, in *20th International Conference on the Physics of Semiconductors*, edited by E. M. Anastassakis and J. D. Joannopoulos (World Scientific, Singapore, 1990), Vol. 3, p. 1755.
- ³³H. R. Philipp and E. A. Taft, *Phys. Rev.* **127**, 159 (1962); **136**, A1445 (1964).
- ³⁴W. C. Walker and J. Osantowski, *Phys. Rev.* **134**, A153 (1964).
- ³⁵R. A. Roberts, D. M. Roessler, and W. C. Walker, *Phys. Rev. Lett.* **17**, 302 (1966).
- ³⁶R. A. Roberts and W. C. Walker, *Phys. Rev.* **161**, 730 (1967).
- ³⁷W. Saslow, T. K. Bergstresser, and M. L. Cohen, *Phys. Rev. Lett.* **16**, 354 (1966).
- ³⁸L. R. Saravia and D. Brust, *Phys. Rev.* **170**, 683 (1968).
- ³⁹W. van Haeringen and H.-G. Junginger, *Solid State Commun.* **7**, 1135 (1969).
- ⁴⁰L. A. Hemstreet, C. Y. Fong, and M. L. Cohen, *Phys. Rev. B* **2**, 2054 (1970).
- ⁴¹F. J. Himpsel, J. F. van der Veen, and D. E. Eastman, *Phys. Rev. B* **22**, 1967 (1980).
- ⁴²M. S. Hybertsen and S. G. Louie, *Phys. Rev. B* **34**, 5390 (1986); *Phys. Rev. Lett.* **55**, 1418 (1985).
- ⁴³R. Hott, *Phys. Rev. B* **44**, 1057 (1991).
- ⁴⁴T. C. Chiang and F. J. Himpsel, in *Numerical Data and Functional Relationships in Science and Technology*, edited by A. Goldmann and E.-E. Koch (Springer, Berlin, 1989), Vol. 23, p. 12.
- ⁴⁵C. D. Clark, P. J. Dean, and P. V. Harris, *Proc. R. Soc. London Ser. A* **277**, 312 (1964).
- ⁴⁶P. J. Dean, E. C. Lightowers, and D. R. Wright, *Phys. Rev.* **140**, A352 (1965).
- ⁴⁷P. Lautenschlager, M. Garriga, L. Viña, and M. Cardona, *Phys. Rev. B* **36**, 4821 (1987).
- ⁴⁸S. Zollner, M. Garriga, J. Humlíček, S. Gopalan, and M. Cardona, *Phys. Rev. B* **43**, 4349 (1991).
- ⁴⁹J. Hartung, L. Å. Hansson, and J. Weber, in *20th International Conference on the Physics of Semiconductors* (Ref. 32), p. 1875; J. Weber and M. I. A. Alonso, *Phys. Rev. B* **40**, 5683 (1989).
- ⁵⁰C. D. Thurmond, *J. Electrochem. Soc.* **122**, 1133 (1975).
- ⁵¹R. A. Forman, W. R. Thurber, and D. E. Aspnes, *Solid State Commun.* **14**, 1007 (1974).
- ⁵²J. Humlíček (private communication).
- ⁵³T. C. Chiang and F. J. Himpsel, in *Numerical Data and Functional Relationships in Science and Technology* (Ref. 19), Vol. 23a, p. 15, and references therein.
- ⁵⁴D. Straub, L. Ley, and F. J. Himpsel, *Phys. Rev. Lett.* **54**, 142 (1985).
- ⁵⁵R. Hulthén and N. G. Nilsson, *Solid State Commun.* **18**, 1341 (1976).
- ⁵⁶G. B. Bachelet, H. S. Greenside, G. A. Baraff, and M. Schlüter, *Phys. Rev. B* **24**, 4745 (1981); C. O. Rodriguez, *Solid State Commun.* **46**, 11 (1983).
- ⁵⁷R. W. Godby, M. Schlüter, and L. J. Sham, *Phys. Rev. Lett.* **56**, 2415 (1986).
- ⁵⁸W. von der Linden and P. Horsch, *Phys. Rev. B* **37**, 8351 (1988).
- ⁵⁹L. Viña and M. Cardona, *Phys. Rev. B* **43**, 2586 (1986).
- ⁶⁰D. E. Aspnes and A. A. Studna, *Phys. Rev. B* **27**, 985 (1983).
- ⁶¹L. Viña, S. Logothetidis, and M. Cardona, *Phys. Rev. B* **30**, 1979 (1984).

Errata

Erratum: Isotope and temperature shifts of direct and indirect band gaps in diamond-type semiconductors [Phys. Rev. B 45, 3376 (1992)]

Stefan Zollner, Manuel Cardona, and Sudha Gopalan

Figure 2 in the original article is wrong. The correct figure is shown below.

